Global phase diagram of one-dimensional graded diatomic elastic chains: a diagrammatic approach to identifying vibrational normal modes

2007 J. Phys.: Condens. Matter 19 026224

(http://iopscience.iop.org/0953-8984/19/2/026224)

INSTITUTE OF PHYSICS PUBLISHING JOURNAL OF PHYSICS: CONDENSED MATTER

J. Phys.: Condens. Matter **19** (2007) 026224 (10pp) doi:10.1088/0953-8984/19/2/026224

Global phase diagram of one-dimensional graded diatomic elastic chains: a diagrammatic approach to identifying vibrational normal modes

J J Xiao[1], K Yakubo[2] and K W Yu[1,3]

[1] Department of Physics, The Chinese University of Hong Kong, Shatin, New Territories, Hong Kong, People's Republic of China
[2] Division of Applied Physics, Graduate School of Engineering, Hokkaido University, N13-W8, Sapporo 060-8628, Japan
[3] Institute of Theoretical Physics, The Chinese University of Hong Kong, Shatin, New Territories, Hong Kong, People's Republic of China

E-mail: jjxiao@phy.cuhk.edu.hk

Received 15 September 2006
Published 15 December 2006
Online at stacks.iop.org/JPhysCM/19/026224

Abstract

We study vibrational normal modes in graded diatomic chains wherein the masses m_1 of one type of atom vary linearly with the gradient c while those of the other type m_2 remain constant, in order to examine the diatomic effect on one-dimensional graded elastic chains. By means of a band overlapping picture—a convenient diagrammatic approach—we found six distinct kinds of vibrational mode, four of which are localized and two extended. Depending on their characteristics, we are also able to categorize these modes into acoustic and optical modes. Furthermore, investigating transitions among these rich normal modes we construct the global phase diagrams of vibrational modes in the ω–c space. All results are verified by numerical calculations in finite size systems.

(Some figures in this article are in colour only in the electronic version)

1. Introduction

In inhomogeneous media, electronic eigenstates or excitations can become spatially localized, as compared to their extended counterparts in homogeneous systems or perfectly crystalline materials with high point group symmetry. The localization phenomena occur mainly due to either interference or potential confinement. Examples in the former case include the Anderson localization of quantum and classical waves [1, 2] and fractons in fractal systems [3], while in the latter case notable examples are impurity states in semiconductors [4, 5], laser cooling [6], pinning of charge-density-waves [7], and electronic confined states in quantum dots [8]. Concomitantly, localization–delocalization (LD) transitions may occur in both of these two cases, alternating macroscopic properties of systems. In terms of understanding the

fundamental nature of localization and managing the spectral bands, there are a wider range of systems under study, such as random media, quasi-periodic systems, meta-materials, as well as graded systems [9]. This topic has been of great interest over the past decades and is an urgent problem associated with the current rapid advancement in nanofabrication techniques. Since new types of localization or the LD transitions may lead to novel functions of materials, it is important to study the localization problem in various systems. In fact, localization properties of waves are deeply related to many applications, ranging from semiconductor-device physics to the random laser [10].

Recently, to find exotic localized modes, we examined in detail vibrational normal modes in graded elastic chains [11] and networks [12]. From simple lattice models it has been shown that novel localized vibrational modes peculiar to graded elastic lattices, named 'gradons', possess an unusual spatial extent and exhibit a new kind of LD transition, offering a fine-tuning spectral functionality. The results provide a way to control localized modes and suggest an efficient method for engineering phonon dispersion in solids. In addition, these discoveries have been successfully applied to manipulate coupled plasmon modes in graded plasmonic crystals, providing a great opportunity to employ a variety of plasmonic gradons in achieving deep-subwavelength optical energy confinement and routing [13]. In particular gradons are relevant to recent exploration of localized vibrational normal modes in optically bound structures [14]. These photonic clusters demonstrate exotic dynamics because of the complicated optical binding forces featuring a gradient [15], which open a new gate for studying elastically inhomogeneous systems by irradiating light illumination.

Previous studies of gradon localization have been focused on monatomic graded systems. While monatomic materials such as simple metals are rather rare in a wide range of actual materials, it is necessary to examine excitations in graded diatomic (or polyatomic) lattices which are well-devised models for designing graded solids. From the non-universal nature of gradons, it can be expected that characteristics of gradons excited in graded diatomic lattices are largely different from those in graded monatomic ones. In this paper, we use both an analytical (diagrammatic) approach and numerical calculations to identify various harmonic vibrational modes of graded diatomic chains (GDCs) and figure out the phase diagram of eigenmodes. Using the graded mass model dramatically simplifies the analysis but retains the underlying physics dominating the dynamics, due to the duality of masses and force constants. Our main goal in this paper is to understand the nature of localized vibrational modes in GDCs and clarify essential differences from gradons in graded monatomic chains by extending the arguments of [11]. In the following section, we present our diatomic model with graded masses and elaborate the diagrammatic approach. This approach has been proven powerful, and helps us to construct the global phase diagrams in section 3. In this section, our analytical predictions are verified by numerical calculations for finite size systems. Finally, we provide a brief summary in section 4.

2. Model and the band overlapping picture: infinite chains

The diatomic model with graded masses, which we study here, is schematically shown in figure 1(a). Two types of atom, namely type-1 and type-2, are alternatively placed in a one-dimensional direction. Masses of type-1 and type-2 atoms are denoted by m_1 and m_2, respectively. The force constants of linear springs connecting type-1 to type-2 atoms and type-2 to type-1 atoms are given by K_1 and K_2, respectively. In our GDC, masses are not constant but vary linearly along the chain. For simplicity, we fix m_2 as a constant, impose a linear decrease in $m_1(n)$, where n denotes the site index for type-1 atom, and assume $K_1 = K_2$. That

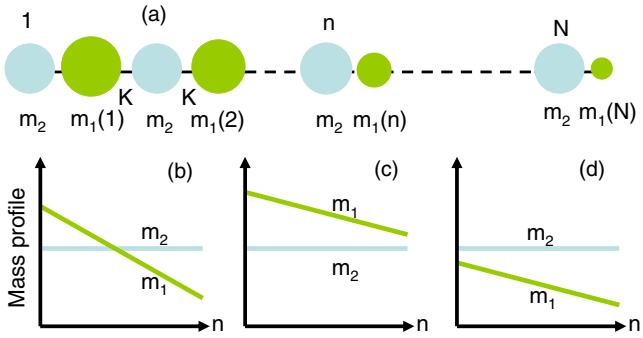

Figure 1. (a) Schematic figure of a graded diatomic elastic chain. $m_2(n)$ remain identical while $m_1(n)$ decrease linearly from $m_1(1)$ to $m_1(N)$. (b)–(d) Typical configurations in the graded profiles of m_1 and m_2 with respect to the cell number n.

is, we employ the following profiles of masses and the force constants:

$$m_1(n) = m_1(1) - c\frac{n-1}{N-1}, \qquad (n = 1, 2, \ldots, N) \tag{1a}$$

$$m_2(n) = m_2, \qquad (n = 1, 2, \ldots, N) \tag{1b}$$

$$K_1 = K_2 = K, \tag{1c}$$

where c gives the strength of the gradient and N denotes the total number of cells which are a pair of type-1 and type-2 atoms. It should be remarked that N can take either a finite or an infinite number. Depending on the parameters $m_1(1)$, m_2 and c, we have three possible situations as depicted in figures 1(b)–(d), namely $m_1(1) \geqslant m_2 > m_1(N)$ (figure 1(b)), $m_1(1) > m_1(N) \geqslant m_2$ (figure 1(c)) and $m_2 > m_1(1) > m_1(N)$ (figure 1(d)). The equations of motion thus read [18, 19]

$$m_1(n)\ddot{u}_n = -K[2u_n - v_n - v_{n+1}], \qquad (n = 1, 2, \ldots, N) \tag{2a}$$

$$m_2(n)\ddot{v}_n = -K[2v_n - u_n - u_{n-1}], \qquad (n = 1, 2, \ldots, N), \tag{2b}$$

where u_n and v_n are, respectively, the displacements of type-1 and type-2 atoms in the nth cell and the derivative is taken with respect to time t.

To make our discussions on GDCs easier, let us first review the well known results of the phonon dispersion in a homogeneous diatomic chain (HDC) with $c = 0$. In such a system, the phonon dispersion relation $\omega(k)$, namely frequency ω versus wavenumber k, has two branches, according to the $+$ and $-$ signs in the following equation [16, 17]:

$$\omega^2_{\mathrm{ac,opt}}(k) = \frac{\omega_0^2}{2}\left[1 \mp \sqrt{1 - \beta^2 \sin^2\frac{ka}{2}}\right], \tag{3}$$

where

$$\omega_0^2 = \frac{2K(m_\mathrm{H} + m_\mathrm{L})}{m_\mathrm{H} m_\mathrm{L}}, \tag{4a}$$

$$\beta^2 = \frac{4m_\mathrm{H} m_\mathrm{L}}{(m_\mathrm{H} + m_\mathrm{L})^2}, \tag{4b}$$

and a is the lattice constant. In this special case, we use m_L and m_H ($\geqslant m_\mathrm{L}$) instead of m_1 and m_2. When $m_\mathrm{L} = m_\mathrm{H}$, the relation (3) becomes equivalent to that of a homogeneous monatomic chain. Normally, the lower frequency acoustic branch ω_ac (the higher frequency optical branch ω_opt) has its lower (upper) and upper (lower) bounds at the zone centre ($k = 0$)

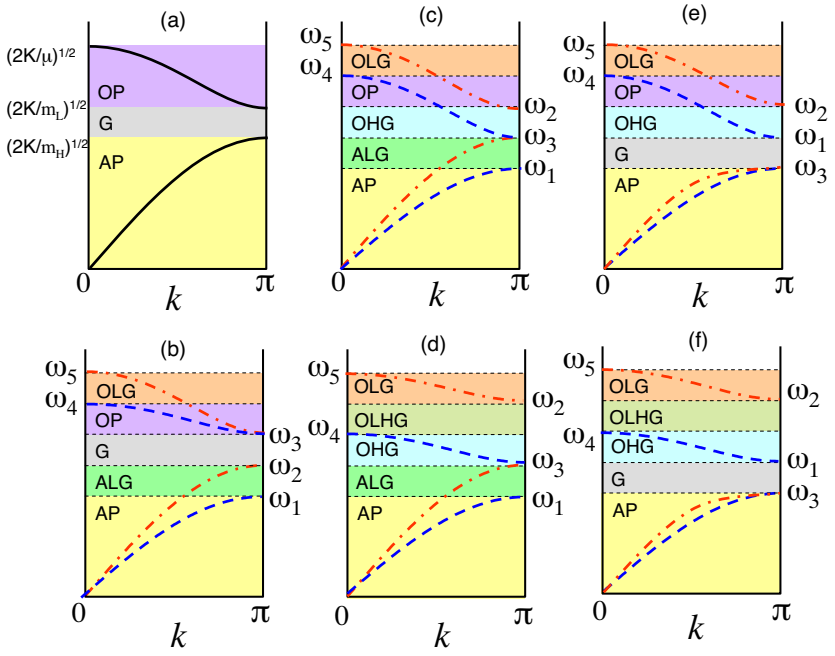

Figure 2. Mode classification by the band overlapping picture. (a) The dispersion relation of a homogeneous diatomic chain with $c = 0$ and (b)–(f) representing cases 1–5 in table 1. Abbreviations in these figures are defined in the text. Only the positive k value of the first Brillouin zone is shown.

and the zone boundary ($k = \pi/a$), respectively. The monotonicity of each dispersion relation is crucial for analysing various modes in a GDC and constructing the global phase diagram by our diagrammatic approach. A typical two-branch dispersion is depicted in figure 2(a) for a HDC. Let us denote such a system as HDC[$m_{\rm L}$, $m_{\rm H}$]. The three band edges in figure 2(a) are determined by the mass ratio $\alpha \equiv m_{\rm H}/m_{\rm L}$ and the effective mass $\mu = m_{\rm L}m_{\rm H}/(m_{\rm L} + m_{\rm H})$. It is worthwhile remarking that the upper bound of the acoustic band is determined only by the heavy mass $m_{\rm H}$, while the lower bound of the optical band depends only on the light one $m_{\rm L}$. We will see later that this is the origin of the vanishing gap when the profile of $m_1(n)$ intersects m_2 in a GDC.

Let us consider vibrational modes in an infinite GDC defined by equation (1) with $N \to \infty$. To this end, we divide the whole GDC into small segments. The size of these segments is so small that the graded masses $m_1(n)$ can be regarded as a constant in each segment, but still infinite. Namely, we regard the whole GDC as the infinite number of infinite homogeneous diatomic chains (segments) with constant m_2 and m_1 depending on segments. Although these segments are connected to each other by the linear springs K, the ratio of the number of these inter-segment springs to that of all the springs included in the whole GDC is infinitesimal. Therefore, we can neglect contributions from these inter-segment couplings to spectral properties of the GDC. In this limit, the original GDC is constructed by isolated segments. Since vibrational modes in the ith segment with constant masses m_1^i and m_2 are completely described by equation (3) with $m_{\rm H} = \max(m_1^i, m_2)$ and $m_{\rm L} = \min(m_1^i, m_2)$, the whole GDC possesses dispersion relations with possible values of m_1^i ranging from $m_1^{\min} = m_1(1) - c$ to $m_1^{\max} = m_1(1)$ simultaneously. It should be noted that the wavenumber k in equation (3) is only locally defined in the GDC because k cannot be a

Table 1. Possible relations between characteristic frequencies ω_1, ω_2, ω_3, ω_4 and ω_5 and corresponding relations in masses m_1 and m_2. Corresponding figures 1, 2, 3, and 5 are also listed in the columns of F 1, F 2, F 3, and F 5, respectively.

Case	Frequency relationship	Mass relationship	F 1	F 2	F 3	F 5
1	$\omega_1 \leqslant \omega_2 < \omega_3 < \omega_4 \leqslant \omega_5$	$m_2 < m_1^{\min}$; $\frac{1}{m_2} \geqslant \frac{1}{m_1^{\min}} - \frac{1}{m_1^{\max}}$	1(c)	2(b)	3(a)	5(b)
2	$\omega_1 < \omega_3 \leqslant \omega_2 \leqslant \omega_4 < \omega_5$	$m_1^{\min} \leqslant m_2 < m_1^{\max}$; $\frac{1}{m_2} \geqslant \frac{1}{m_1^{\min}} - \frac{1}{m_1^{\max}}$	1(b)	2(c)	3(a)	5(c)
3	$\omega_1 < \omega_3 < \omega_4 \leqslant \omega_2 < \omega_5$	$m_1^{\min} \leqslant m_2 < m_1^{\max}$; $\frac{1}{m_2} < \frac{1}{m_1^{\min}} - \frac{1}{m_1^{\max}}$	1(b)	2(d)	3(a)	5(d)
4	$\omega_3 \leqslant \omega_1 \leqslant \omega_2 \leqslant \omega_4 \leqslant \omega_5$	$m_1^{\max} \leqslant m_2$; $\frac{1}{m_2} \geqslant \frac{1}{m_1^{\min}} - \frac{1}{m_1^{\max}}$	1(d)	2(e)	3(b)	5(e)
5	$\omega_3 \leqslant \omega_1 < \omega_4 \leqslant \omega_2 < \omega_5$	$m_1^{\max} \leqslant m_2$; $\frac{1}{m_2} < \frac{1}{m_1^{\min}} - \frac{1}{m_1^{\max}}$	1(d)	2(f)	3(b)	5(f)

conserved quantity due to a lack of translational symmetry. In a HDC, the spectral band can be characterized by three band edge frequencies as seen in figure 2(a), namely $\sqrt{2K/\mu}$, $\sqrt{2K/m_{\mathrm{L}}}$ and $\sqrt{2K/m_{\mathrm{H}}}$. From the monotonicity of the dispersion relation, the spectrum of the whole GDC has the following five characteristic frequencies corresponding to these three frequencies:

$$\omega_1 = \sqrt{\frac{2K}{m_1^{\max}}} \tag{5a}$$

$$\omega_2 = \sqrt{\frac{2K}{m_1^{\min}}} \tag{5b}$$

$$\omega_3 = \sqrt{\frac{2K}{m_2}} \tag{5c}$$

$$\omega_4 = \sqrt{2K\left[\frac{1}{m_1^{\max}} + \frac{1}{m_2}\right]} \tag{5d}$$

$$\omega_5 = \sqrt{2K\left[\frac{1}{m_1^{\min}} + \frac{1}{m_2}\right]}. \tag{5e}$$

Depending on the relation between masses $m_1^{\min}$, $m_1^{\max}$ and m_2, we have five possible relationships between $\omega_1, \omega_2, \ldots, \omega_5$ as shown in table 1. We discuss in detail the spectral property and mode profiles in the case of $\omega_1 \leqslant \omega_2 < \omega_3 < \omega_4 \leqslant \omega_5$ corresponding to $m_2 < m_1^{\min}$ and $1/m_2 \geqslant 1/m_1^{\min} - 1/m_1^{\max}$ ('case 1' in table 1) as an example. This situation is illustrated in figure 2(b). From the viewpoint that the whole GDC is constructed from a number of segmental HDCs, the GDC has 'local' acoustic dispersions falling between the (blue) dashed line (ranging from 0 to ω_1) and the (red) dash–dotted line (ranging from 0 to ω_2). For the optical branch, the local optical dispersions lie in the region between the (blue) dashed line (ranging from ω_4 to ω_3) and the (red) dash–dotted line (ranging from ω_5 to ω_3). Therefore, there exist vibrational eigenmodes in the frequency ranges from 0 to ω_2 and ω_3 to ω_5. We have the band gap between ω_2 and ω_3 and the highest band edge at $\omega = \omega_5$. In the frequency region $[0, \omega_1]$, all acoustic dispersions of any segmental HDCs share this region. This implies that all segmental HDCs can vibrate at a common frequency. These equi-frequency modes construct spatially extended vibrational excitations in the GDC. We call such extended modes over the chain 'acoustic phonons' (APs) after conventional terminology, though eigenmodes in this region are somewhat different from the usual acoustic phonons in homogeneous lattices

because the (local) wavelength in our AP depends on the position in the GDC. In the frequency region between ω_1 and ω_2, however, some of the dispersion relations of HDCs (i.e. local dispersions in the GDC) do not occupy part of this region. Let us consider a mode belonging to a specific frequency ω within the region $[\omega_1, \omega_2]$. Segmental HDCs with masses m_1^i less than $m^* \equiv 2K/\omega^2$ can vibrate with this frequency. The frequency ω is, however, beyond the upper band edge of the acoustic branch of segmental HDCs with masses m_1^i larger than m^*. This implies that the vibrational mode of ω in the GDC has finite amplitudes only in a part with $m_1(n) < m^*$, namely localized in a lighter part of the GDC. We call these modes 'acoustic light gradons' (ALGs) after the gradon [11] excited in graded monatomic lattices (see figure 2(b)). This band overlapping picture can be also applied to the optical band. The frequency region between ω_3 and ω_4 is shared by all optical dispersions of any segmental HDCs. Thus, we can expect extended 'optical phonons' (OPs) in the GDC. On the contrary, the local dispersions only partially occupy the frequency region $[\omega_4, \omega_5]$, which implies that optical modes at frequencies contained in this region are localized in lighter parts of the GDC as in the acoustic case. These modes are referred to as 'optical light gradons' (OLGs). From these arguments based on the band overlapping picture, we can summarize the characteristics of vibrational modes in the GDC satisfying the condition $\omega_1 \leqslant \omega_2 < \omega_3 < \omega_4 \leqslant \omega_5$ as depicted in figure 2(b).

For the other four cases listed in table 1, it is also efficient to apply our diagrammatic approach for classifying vibrational modes in the GDC. Our results are summarized in figures 2(b)–(f). It should be noted that the band gap disappears for systems with mass profiles like figure 1(b). This is because we have a band gap when the heaviest mass among lighter masses (m_{L}) of HDCs is less than the lightest mass among heavier masses (m_{H}). If the profile of $m_1(n)$ intersects m_2, these two masses coincide, which leads to the vanishing gap. In figures 2(c)–(f), we see the region of 'optical heavy gradons' (OHGs). These modes are localized in heavier parts of the GDC. In the case of figure 2(c), for example, the optical dispersions of the segmental HDCs with m_1^i less than m_2 do not fully occupy this region. This shows that optical vibrational modes with a frequency ω satisfying $\omega_2 > \omega > \omega_3$ do not exist in HDCs with $m_i < 2K/\omega^2$ and the eigenmode belonging to the frequency ω is localized in the heavier part with $m_1(n) > 2K/\omega^2$ in the GDC. The 'optical light-heavy gradons' (OLHGs) found in figures 2(d) and (f) are localized in spatial parts with intermediate $m_1(n)$. In contrast to the fact that all types of gradons discussed so far are localized by half in the GDC, i.e. localized in a lighter half or a heavier half, modes in the OLHG region are completely confined within the GDC. For a frequency ω between ω_2 and ω_4 in figure 2(d) or (f), segmental HDCs with m_1^i satisfying $\omega > \sqrt{2K(1/m_1^i + 1/m_2)}$ cannot vibrate, because the upper optical band edges for these HDCs are less than the frequency ω. Also, HDCs with $m_1^i < 2K/\omega^2$ have no vibrational modes at this frequency, because the lower optical band edges exceed the frequency ω. Therefore, the eigenmode with ω in the GDC should be localized in the spatial region of $2K/\omega^2 < m_1(n) < (\omega^2/2K - 1/m_2)^{-1}$.

3. Global phase diagrams and numerical results

By the characteristic frequencies defined in equations (5*a*)–(5*e*) and the diagrammatic scheme, we are able to construct phase diagrams of vibrational modes in the ω–c space, as shown in figure 3. The horizontal axis of these figures represents the strength of gradient c scaled by $m_1^{\max}$. This quantity varies from 0 to 1 so that $m_1(n)$ is always positive and decreases from the left-hand side to the right-hand side. Five lines in these figures indicate the characteristic frequencies defined by equation (5) as functions of $c/m_1^{\max}$. Figure 3 clearly shows that there exist rich phases, dubbed in this work as acoustic phonon (AP), acoustic light gradon (ALG),

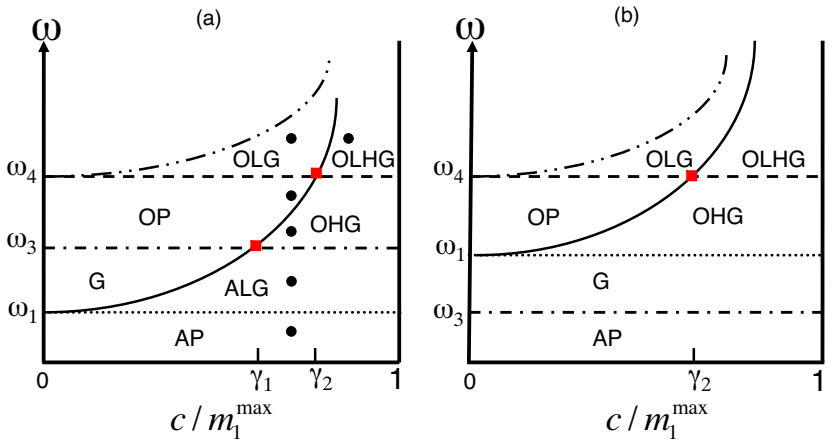

Figure 3. Global phase diagrams for graded diatomic chains with (a) $m_1^{\max} > m_2$ and (b) $m_1^{\max} < m_2$ obtained by the band overlapping picture. The five curves represent $\omega_1 = \sqrt{2K/m_1^{\max}}$ (· · · · · ·), $\omega_2 = \sqrt{2K/(m_1^{\max} - c)}$ (——), $\omega_3 = \sqrt{2K/m_2}$ (— · —), $\omega_4 = \sqrt{2K[1/m_1^{\max} + 1/m_2]}$ (– – –) and $\omega_5 = \sqrt{2K[1/(m_1^{\max} - c) + 1/m_2]}$ (— · · —), respectively. Notice that ω_2 and ω_5 asymptotically meet at $c/m_1^{\max} = 1$.

optical phonon (OP), optical light gradon (OLG), optical heavy gradon (OHG) and optical light-heavy gradon (OLHG). The gap (G) appears for $m_1^{\max} > m_2$ and $c/m_1^{\max} < \gamma_1 (\equiv 1 - m_2/m_1^{\max})$ (figure 3(a)) or for $m_1^{\max} < m_2$ (figure 3(b)). In both parts of 3, the horizontal line of $\omega = \omega_4$ (dashed line) intersects the line of $\omega = \omega_2(c)$ (solid line) at $c/m_1^{\max} = \gamma_2 \equiv 1 - m_2/(m_1^{\max} + m_2)$ (as marked by ■). In figure 4, we show the various normal modes at several representative points (marked as ●) in the phase diagram of figure 3(a). These modes are calculated by diagonalizing the dynamical matrices for equation (2) with $N = 500$, which are consistent with the mode profiles predicted in the preceding section for infinite GDCs. To complement our results, we present the density of states (DOS) of an infinite GDC. Based on the idea that the GDC is divided into small segments of HDCs, the DOS is given by

$$D_{\mathrm{GDC}}(\omega) = \frac{1}{c} \int_{m_1^{\min}}^{m_1^{\max}} D_{\mathrm{HDC}}(m_1, m_2; \omega)\, \mathrm{d}m_1, \tag{6}$$

where

$$D_{\mathrm{HDC}}(m_1, m_2; \omega) = \frac{2\omega}{\pi} \mathrm{Re} \left\{ \frac{|\omega_0^2 - 2\omega^2|}{\left[(\omega_0^2 - \omega^2)[\omega^2 - \omega_{\mathrm{opt}}^2(\pi/a)][\omega^2 - \omega_{\mathrm{ac}}^2(\pi/a)]\omega^2\right]^{\frac{1}{2}}} \right\} \tag{7}$$

is the analytical DOS for a HDC$[m_1, m_2]$ [16, 17]. Here, the frequencies ω_0, ω_{ac} and ω_{opt} are defined by equations (3) and (4) with $m_{\mathrm{L}} = \min(m_1, m_2)$ and $m_{\mathrm{H}} = \max(m_1, m_2)$. Results for several combinations of $m_1(1)$ and c are shown in figure 5 where $m_2 = 1$. The DOS curves indicate complicated but interesting behaviours, which agree well with the numerical calculations (not shown here) for finite GDCs. The different modes and their transitions labelled in figure 2 are clearly reflected in the DOS curves with some singularities (for those that is not remarkable, we added a downward arrow above). In figure 5(b), for example, we have acoustic phonon (AP) modes in the frequency region of $0 < \omega \leqslant \omega_1$, and acoustic light gradon (ALG) modes for $\omega_1 < \omega \leqslant \omega_2$. It is clearly seen that GDC retain the two-band structure but the gap may vanish when the profiles of $m_1(n)$ and m_2 cross each other, as we remarked previously. Re-

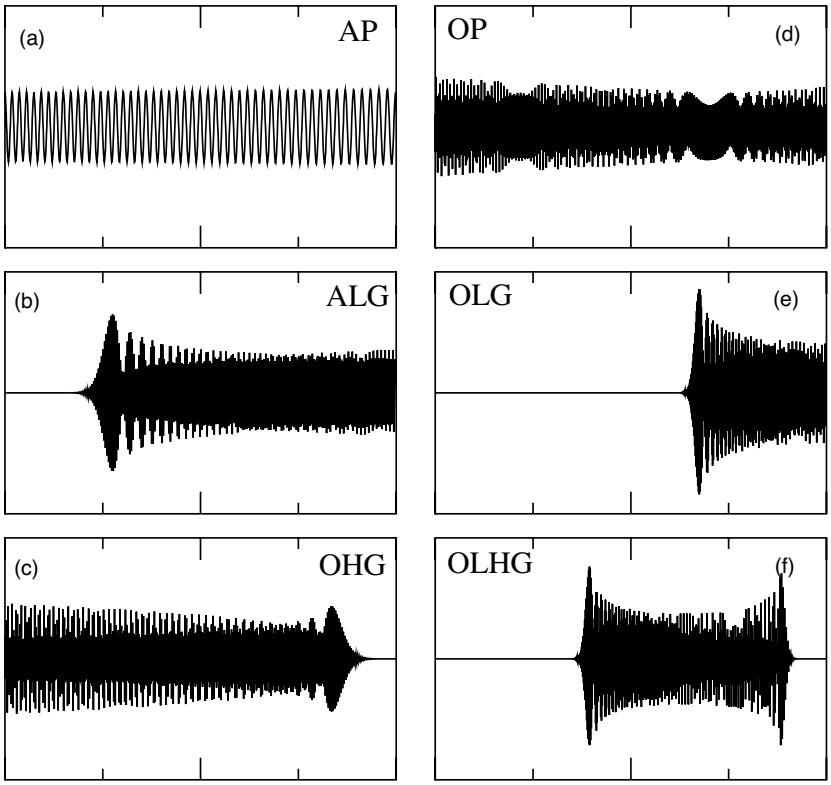

Figure 4. Numerically calculated normal modes at the representative points (●) indicated in the phase diagram of figure 3(a). The system size N in numerical calculations is 500.

entrant transitions as 'extended' → 'localized' → 'extended' modes with increasing frequency are features of the GDC. The correspondence between figures 1, 2, 3 and 5 are shown in table 1.

4. Summary

In conclusion, we study the nature of vibrational modes excited in one-dimensional graded diatomic chains (GDCs) and obtain the global phase diagram of modes. We identify the various mode types and transitions among them by an efficient method in the sprit of band overlaps of segmental homogeneous diatomic chains (HDCs) into which the whole GDC is divided. The diagrammatic approach can tell us directly how the gradient in masses can affect the spectral properties and mode patterns. In contrast to the case of single band models [11], we show rich varieties of vibrational excitations, especially localized modes (gradons) in a GDC. The results we obtained not only provide deep insight into vibrational excitations in GDCs, assisting the design and exploitation of unique wave functional materials—graded functional materials [9], which are seeing dramatically increasing potential applications ranging from rocket heat shields to human implants—but also shed new light on the dynamics of various optically bounded clusters and suggest a new and powerful way towards phonon band manipulation.

In contrast to HDCs, a single band (i.e. zero gap) spectrum is possible in GDCs when any part of $m_1(n)$ becomes equal to m_2. Although m_2 is set to be constant for any cell n in our

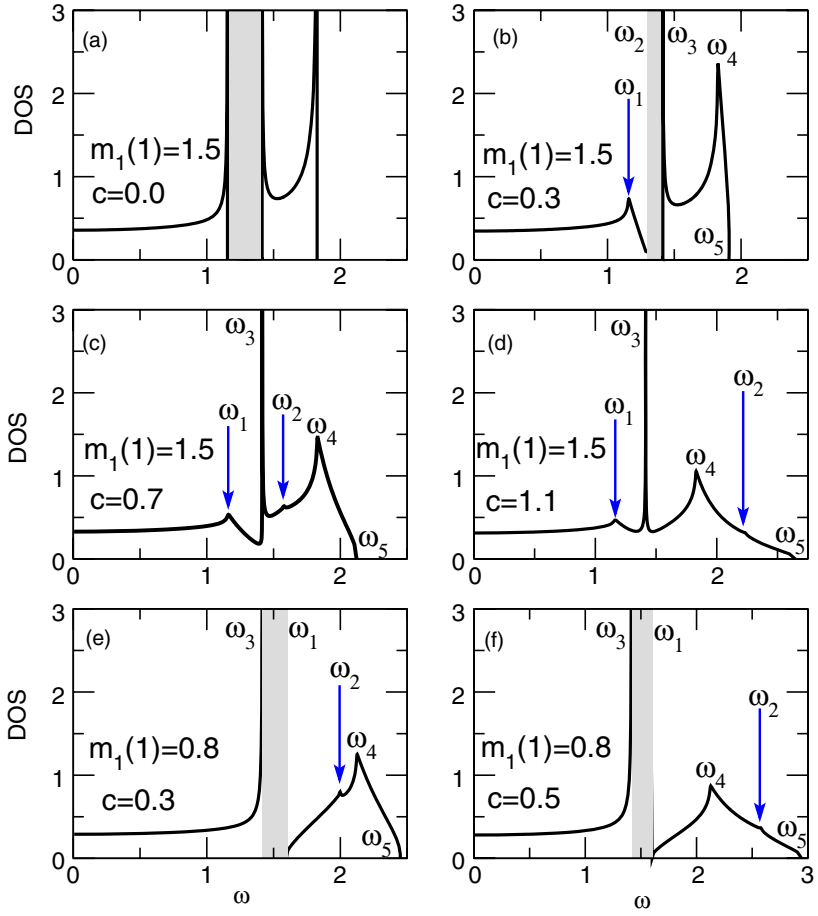

Figure 5. Densities of states (DOSs) for vibration modes in typical graded diatomic chains (GDCs). The largest mass $m_1(1)$ at the left extremity and gradient coefficient c are indicated in each panel. (a) The DOS for a homogeneous diatomic chain. (b)–(f) The representative DOSs for GDCs corresponding to cases 1–5 in table 1, respectively.

present work, our findings provide rich information for more general GDCs with graded $m_1(n)$ and $m_2(n)$. For instance, it can be expected that the acoustical-optical gap vanishes as long as general profiles of $m_1(n)$ and $m_2(n)$ cross each other. In addition to the discovery of the various localized modes, named gradons, different from localization due to impurity, disorder, nonlinear effects, or finite size effects [20, 21], we particularly emphasize the efficiency of the diagrammatic approach based upon the band overlapping picture. This approach is also applicable for any type of inhomogeneous infinite system which can be regarded as an ensemble of homogeneous segments. Due to the non-universal nature of the localized modes in GDCs, further interesting results are anticipated for polyatomic lattices in higher dimensions if a gradient is introduced along a certain direction. It is also possible to extend our method to anisotropic lattices [24], lattices with second-neighbour interactions [25] and lattices with on-site potentials [26]. In view of the fact that such a system demonstrates rich varieties of excitations, it is rewarding to explore phonon-polaritons associated with these lattice vibrations coupled to electromagnetic waves.

Our theoretical predictions presented here can be confirmed experimentally, for example by investigating vibrational modes in optically bound chains [15]. A plasmonic waveguide consisting of a chain of metallic nanoshells [22] may also demonstrate a near field electromagnetic analogy to our model. It is also possible to develop much simpler experiments [23] to verify the reported results.

Acknowledgments

This work was supported in part by the RGC Earmarked Grant of the Hong Kong SAR Government (KWY), and in part by a Grant-in-Aid for Scientific Research from the Japan Society for the Promotion of Science (no. 16360044).

References

[1] Altshuler B L, Lee P A and Webb R A 1991 *Mesoscopic Phenomena in Solids* (Amsterdam: North-Holland)
[2] Sheng P 1995 *Introduction to Wave Scattering, Localization and Mesoscopic Phenomena* (New York: Academic)
[3] Nakayama T, Yakubo K and Orbach R L 1994 *Rev. Mod. Phys.* **66** 381
[4] Callaway J 1964 *J. Math. Phys.* **5** 783
[5] Faulkner R A 1968 *Phys. Rev.* **175** 991
[6] Phillips W D 1998 *Rev. Mod. Phys.* **70** 721
[7] Gruner G and Zettl A 1985 *Phys. Rep.* **119** 117
[8] Ledentsov N N, Ustinov V M, Shchukin V A, Kop'ev P S, Alferov Z I and Bimberg D 1998 *Semiconductors* **32** 343
[9] Huang J P and Yu K W 2006 *Phys. Rep.* **431** 87
[10] Lawandy N M, Balachandran R M, Gomes A S L and Sauvain E 1994 *Nature* **368** 436
[11] Xiao J J, Yakubo K and Yu K W 2006 *Phys. Rev.* B **73** 054201
[12] Xiao J J, Yakubo K and Yu K W 2006 *Phys. Rev.* B **73** 224201
[13] Xiao J J, Yakubo K and Yu K W 2006 *Appl. Phys. Lett.* **88** 241111
[14] Ng J and Chan C T 2006 *Opt. Lett.* **31** 2583
[15] Ng J, Chan C T, Sheng P and Lin Z F 2006 *Opt. Lett.* **30** 1956
[16] Wu S Y and Taylor P L 1969 *Phys. Rev.* **181** 1136
[17] Sen P N and Hartmann W M 1974 *Phys. Rev.* B **9** 367
[18] Kittel C 1996 *Introduction to Solid State Physics* 7th edn (New York: Wiley)
[19] Ziman J M 1969 *Principles of the Theory of Solids* (New York: Cambridge University Press)
[20] Kiselev S A, Bickham S R and Sievers A J 1994 *Phys. Rev.* B **50** 9135
[21] Franchini A, Bortolani V and Wallis R F 2002 *J. Phys.: Condens. Matter* **14** 145
[22] Prodan E, Radloff C, Halas N J and Nordlander P 2003 *Science* **302** 419
[23] Hladky-Henniona A, Allan G and de Billy M 2005 *J. Appl. Phys.* **98** 054909
[24] Duncan D B, Eilbeck J C, Walshaw C H and Zakharov V 1991 *Phys. Lett.* A **158** 107
[25] Tew R B and Wattis J A D 2001 *J. Phys. A: Math. Gen.* **34** 7163
[26] Wattis J A D 1998 *J. Phys. A: Math. Gen.* **31** 3301